ATOMIZATION OF HIGH-VISCOSITY AND NON-NEWTONIAN FLUIDS BY PRE-MIXING

Tom Baker,[1,2] Michele Negri,[2] & Volfango Bertola[1,*]

[1]*Laboratory of Technical Physics, School of Engineering, University of Liverpool, Liverpool, L69 3GH, United Kingdom*

[2]*DLR - German Aerospace Center, Institute of Space Propulsion, Lampoldshausen, Langer Grund, 74239 Hardthausen, Germany*

*Address all correspondence to: Volfango Bertola, Laboratory of Technical Physics, School of Engineering, University of Liverpool, Liverpool, United Kingdom, L69 3GH, E-mail: Volfango.Bertola@liverpool.ac.uk

Original Manuscript Submitted: mm/dd/yyyy; Final Draft Received: mm/dd/yyyy

A novel concept of spray generator is described, which combines aerodynamic and mechanical liquid breakup to achieve liquid atomisation. In particular, the concept of air-blast (effervescent) atomiser is combined with the well-known stretch-and-fold mechanism commonly used in mixing high-viscosity fluids. The proposed technology is suitable to generate sprays of high-viscosity and non-Newtonian fluids, and in general enables liquid atomisation at significantly lower pressures than conventional nozzles. A prototype spray generator based on this concept was designed, built, and tested with two fluids: an aqueous glycerol solution and a a Carbopol polymer dispersion in water. For each fluid, the spray generator performance was studied changing the mass flow rates of fluid and air, and the rotation speed. Shadowgraph images of the spray were analysed with a custom Matlab application to determine the cone angle and the drop size distribution.

KEY WORDS: *select up to 10 key terms for a search on your document*

1. INTRODUCTION

Atomization of high-viscosity fluids, such as heavy oil, is technically challenging because conventional nozzles require significantly high pressures in order to achieve the desired spray characteristics. The atomization of complex fluids is challenging as well, being influenced from the fluid microstructure: some type of complex fluids are atomized quite easily, while others are extremely difficult to break up into fine

droplets. The parameters used to describe the atomization of Newtonian fluids (viscosity, surface tension and density) are not sufficient to predict the atomization of complex fluids. A good example is given by the comparison between two shear thinning non-Newtonian gels (Ethanol + 3.5 % Methocel 311 and Ethanol + 10 % COK 84) with similar viscosity curves (Negri et al., 2013). The shear rates in the injector reached high values (up to 10^4 s^{-1}), leading to a strong decrease of the viscosity of the fluids in the nozzle. Thus, a good atomization is expected for both fluids. However, the experimental observations show instead that one fluid atomizes well, while the other produces elongated ligaments which do not disrupted into droplets. The instability and breakup mechanisms of liquid jets and sheets is inflenced from the fluid microstrusture (Brenn and Plohl, 2017). Complex fluid in which the microstructure is composed from elongated molecules, for example linear polymer solution and other polymeric liquids, proved difficult to atomize (Negri and Ciezki, 2017; Schütz et al., 2004; Thompson and Rothstein, 2007). Such fluids form stable viscoelastic films and ligaments, which prevent a proper atomization.

The capillary breakup of non-Newtonian fluids is an active subject of investigation (Clasen et al., 2012; German and Bertola, 2010a; Plog et al., 2005; Smith et al., 2010), and is poorly understood to date in comparison with the established theory for Newtonian fluids (Lin and Reitz, 1998). However, a growing number of practical or industrial applications now require dispensing of complex fluids with highly non-Newtonian behaviour, in the form of either single droplets or sprays. Examples include drop-on-demand printheads for additive manufacturing, nozzles for rocket gel propellants, fuel injectors for thermodynamic engines using heavy oils, dispensers used in food processing, and many others.

To facilitate the aerodynamic capillary breakup hence the formation of sprays from high-viscosity and non- Newtonian fluids, different technological approaches can be used. Common methods to enhance the atomization of these fluids are the use of air-blast (effervescent) nozzles, where spray generation is assisted by air injection (Broniarz-Press et al., 2010; Rahimi and Natan, 2006), swirl injector nozzles, where the liquid breakup is improved by increasing inertial effects (Yang et al., 2012), and close-coupled atomization, where the fluid jet is disrupted by the direct impact of high–speed jets of a carrier gas just outside the nozzle tip (Mates and Settles, 2005). Recently, sprays of pure glycerin with droplets having diameters below 20 μm were obtained using a Venturi-vortex twin–fluid swirl nozzle atomizing at room temperature (García et al., 2017). However, these high-viscosity and non-Newtonian liquid atomization technologies are still at an early stage of development to date, and their performance is strongly dependent on non-Newtonian effects such as normal stresses, and the yield stress.

This paper introduces an atomization device, based on an alternative concept, which is suitable for high-viscosity and non-Newtonian fluids. The proposed technology combines air injection and swirl with mechanical breakup of the fluid inside the nozzle, achieved through a sequence of stretch-and-fold steps, similar to the well-known approach to mix high-viscosity fluids. This peculiar design was inspired by an industrial mixing apparatus used to produce large quantities of emulsions in the food industry (Akay et al., 2002; Brown et al., 2012). A proof-of-concept prototype of the pre-mixed spray generator was tested with two fluids: a glycerol solution, which has a viscosity significantly higher than water, and a Carbopol polymer dispersion in water, which exhibits viscoplastic behaviour. Results confirm the effectiveness of the proposed atomization process and provide a guide for the optimisation of design and operation parameters.

2. EXPERIMENTAL SETUP AND PROCEDURE

2.1 Spray generator

Figure 1 displays the atomizer assembly (Bertola, 2016). Air (or any carrier gas) and the viscous fluid are injected separately into the gap between two concentric cylinders, one of which is rotating. The inner surface of the outer cylinder (32 mm o.d.; 20 mm i.d.) and the outer surface of the inner cylinder (19 mm o.d.) are shaped in such a way as to form a sequence of narrow gaps (0.5 mm) alternating with larger chambers (15 mm length, 3 mm width and 6 mm height), obtained by milling longitudinal cavities in the outer wall of the inner cylinder and the inner wall of the outer cylinder, respectively. This pattern is intrinsically modular, and can be extended indefinitely in the axial direction using longer cylinders, provided the rotor is adequately supported to avoid vibrations that may cause contact between the gap walls.

The inner cylinder is prolonged into a shaft, mounted on two bearings inserted directly into the extension of the outer cylinder. The outer cylinder terminates with a flange to mount the driving mechanism, directly connected to the rotor. Two threaded fittings in the outer casing serve to supply compressed air and the liquid to spray, with the air intake placed upstream to prevent the liquid from reaching the support bearings. As the air-fluid mixture is forced through the narrow gaps, it experiences large shear rates, stretching the fluid element; these stretched filaments are then mixed with air in the larger section. The

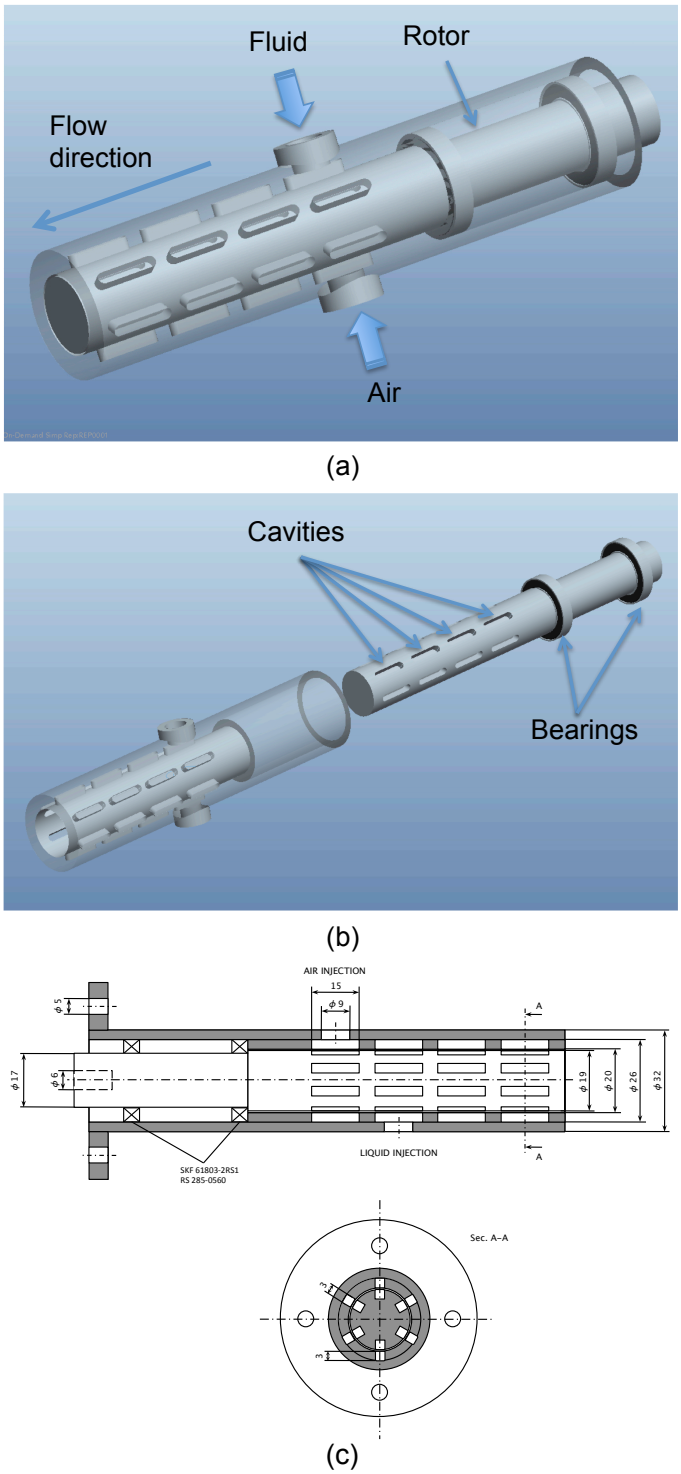

FIG. 1: Atomizer assembly: (a) see–through view; (b) exploded view; (c) longitudinal and axial cross-sections.

stretch-and-fold mechanism takes place when the air-fluid mixture moves between two consecutive cavities, both in the axial and in the tangential direction as the inner cylinder rotates. In the present design, the gap between the concentric cylinders is 0.5 mm, resulting into a hydraulic diameter of 1 mm.

2.2 Fluids preparation and characterization

The test fluids used in the present work were a 65% (w/w) glycerol solution in de-ionised water, having a density of 1170 kg/m^3 and a viscosity of 15 mPa s, and a 0.25% (w/w) Carbopol 980 dispersion in the same de-ionized water and neutralised to pH 7 by adding aqueous NaOH solution (30% w/w), with a density of approximately 1000 kg/m^3 and a yield stress magnitude of 60 Pa. The glycerol solution viscosity was measured with a Haake Mars rotational rheometer equipped with a cone-plate sensor (35 mm diameter and 2° gap angle), used in a controlled rate operation mode across the shear rate range between 0 and 100 s^{-1}. The same rheometer, equipped with a plane-plane sensor having a diameter of 35 mm and a gap of 1 mm, was used in controlled stress mode to measure the yield stress of the Carbopol dispersion. Sandpaper was glued on both the rotating an the fixed surface in order to avoid wall slip effects. The yield point of the viscoplastic gel was determined by fitting the flow curve obtained for shear stresses above the yield point with the Herschel-Bulkley model

$$\tau = \tau_0 + K\dot{\gamma}^n \tag{1}$$

where τ is the shear stress, τ_0 is the yield stress, $\dot{\gamma}$ is the shear rate, K is the consistency index, and n is the flow index. The resulting Herschel-Bulkley fit was then extrapolated to $\dot{\gamma} = 0$ to obtain the magnitude of the yield stress, which is consistent with values reported in the reference literature (Rogers and Barnes, 2001).

The equilibrium surface tension of the glycerol solution was measured with a Kruss EasyDyne tensiometer equipped with a De Nouy ring. Unlike the surface tension of pure liquids, which has an exact definition, the concept of surface tension for viscoplastic fluids is somewhat controversial and is poorly understood to date (Fuller and Vermant, 2012; Jorgensen et al., 2015). Whilst most authors assume the surface tension of Carbopol gels identical to that of water, a systematic investigation on the measurements of the surface tension of viscoplastic fluids suggests that Carbopol gels have a surface tension of approximately 0.066 N/m, irrespective of their yield stress (Boujlel and Coussot, 2013); this value is almost 10%

smaller than that of pure water at ambient temperature.

2.3 Experimental setup and procedure

A schematic layout of the experimental setup is displayed in Figure 2. The rotary atomiser is connected to a DC motor, to allow continuous regulation of the rotation speed, which is measured by a laser tachometer aligned with the motor shaft. The viscous fluid supply is provided by a hydraulic piston cylinder, while the carrier gas is pressurized nitrogen. The nitrogen and the viscous fluid pressures were measured by means of piezo-resistive pressure sensors, connected between the end of the delivery tubes and the injector casing. A volumetric flow meter measured the flow rate of nitrogen, which was then converted into the actual mass flow rate using the pressure and temperature measurements, while the glycerol solution and the Carbopol gel mass flow rates were calculated from the piston speed.

Images of the spray were captured by a CCD camera (PCO2000) with a resolution of 2048x2048 pixels, corresponding to 78 μm/pixel, and a frame rate of 7 fps; the camera was connected to the control PC by firewire cable. Back-to-front illumination was provided by a light source equipped with a shadowgraph lens to ensure parallel illumination in the entire field of view.

Glycerol solution sprays had mass flow rates of fluid in the range between 4.6 g/s and 12.96 g/s, while the nitrogen flow rates were between 5.53 g/s and 10.87 g/s; the corresponding liquid to gas ratios ranged

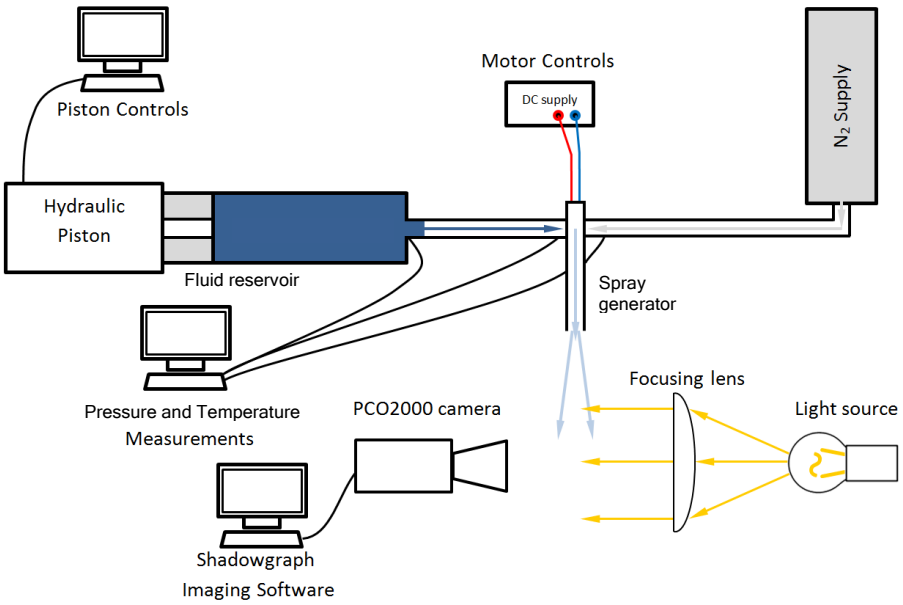

FIG. 2: Schematic of the experimental setup.

from 0.53 to 2.15. A total of 16 tests were carried out, with rotation speeds of between 1000 rpm and 2000 rpm. In the case of Carbopol gel sprays, the mass flow rates of fluid was varied in the range between 2.09 g/s and 10.94 g/s, while the nitrogen flow rates were between 3.2 g/s and 6.77 g/s; the corresponding liquid to gas mass flow ratios ranged from 0.48 to 3.06. A total of 26 tests were carried out, with rotation speeds of between 1000 rpm and 2500 rpm.

2.4 Image processing

Because of the relatively large size of drops produced by this prototype atomiser, conventional laser diagnostic instruments could not be used. However, an initial assessment of the drop size distribution can be obtained by digital image processing of shadowgraph movies. The first image of each movie was subtracted from all subsequent frames to remove the backround. The intensity values of the resulting grayscale images were mapped so that 1% of data were saturated at low and high intensities to enhance contrast. Then each frame was thresholded and converted to binary image using Otsu's method (Otsu, 1979), which chooses the threshold to minimize the interclass variance of the black and of the white pixels. Finally, the algorithm removes any small objects with a size smaller than two pixels, in order to clear the traces left by droplets out of the focal plane, and to fill holes generated by the previous operations.

The drop search algorithm identifies the connected regions in the black and white image, i.e., those

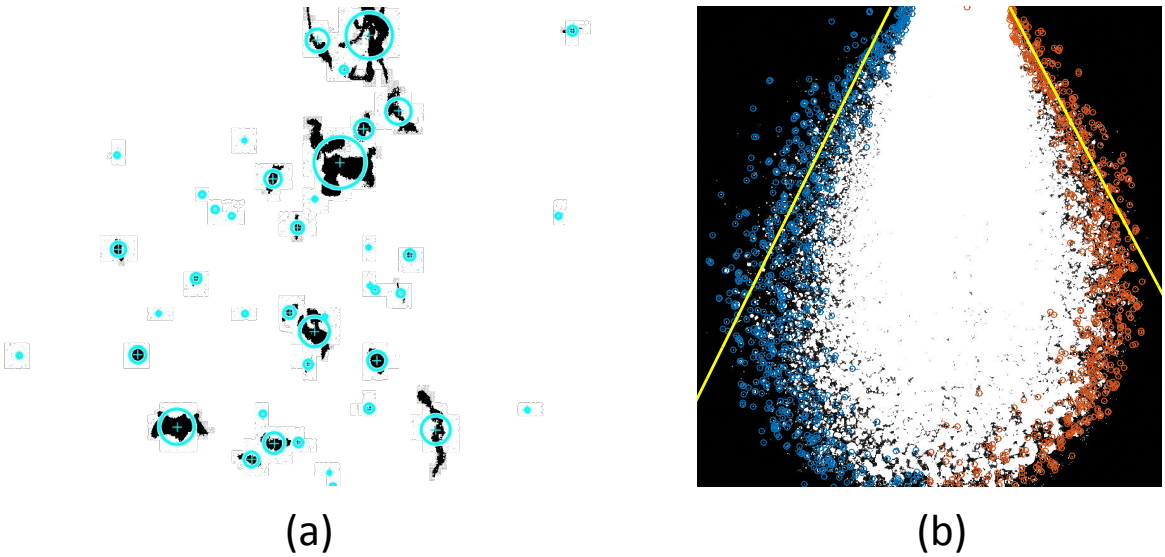

FIG. 3: Drop size distribution analysis (a), where circles are centered in the centroids of the connected regions of the image and have the same area; identification of spray boundary to calculate the cone angle (b).

regions containing pixels which have at least one neighbouring pixel of the same value. To avoid the higher-density region of the spray near the nozzle, where drops may be merged into a same connected region, the drop search is carried out only in the bottom two-thirds of the image. The equivalent diameter of drops was then calculated as $D_{eq} = \sqrt{4A/\pi}$, where A is the area of the connected region. Figure 3a displays an example of the image processing outcome, where irregular lumps of Carbopol gel are converted into circles having the same area.

The spray cone angle was measured from overlay images of several frames, as shown in figure 3b. Spray edges were identified as the points of maximum intensity gradient on each row of the digital image; the straight lines corresponding to the spray cone surface are the least-squares best fit of edge points with the maximum correlation coefficient. This method proved effective in case of glycerol-water mixture

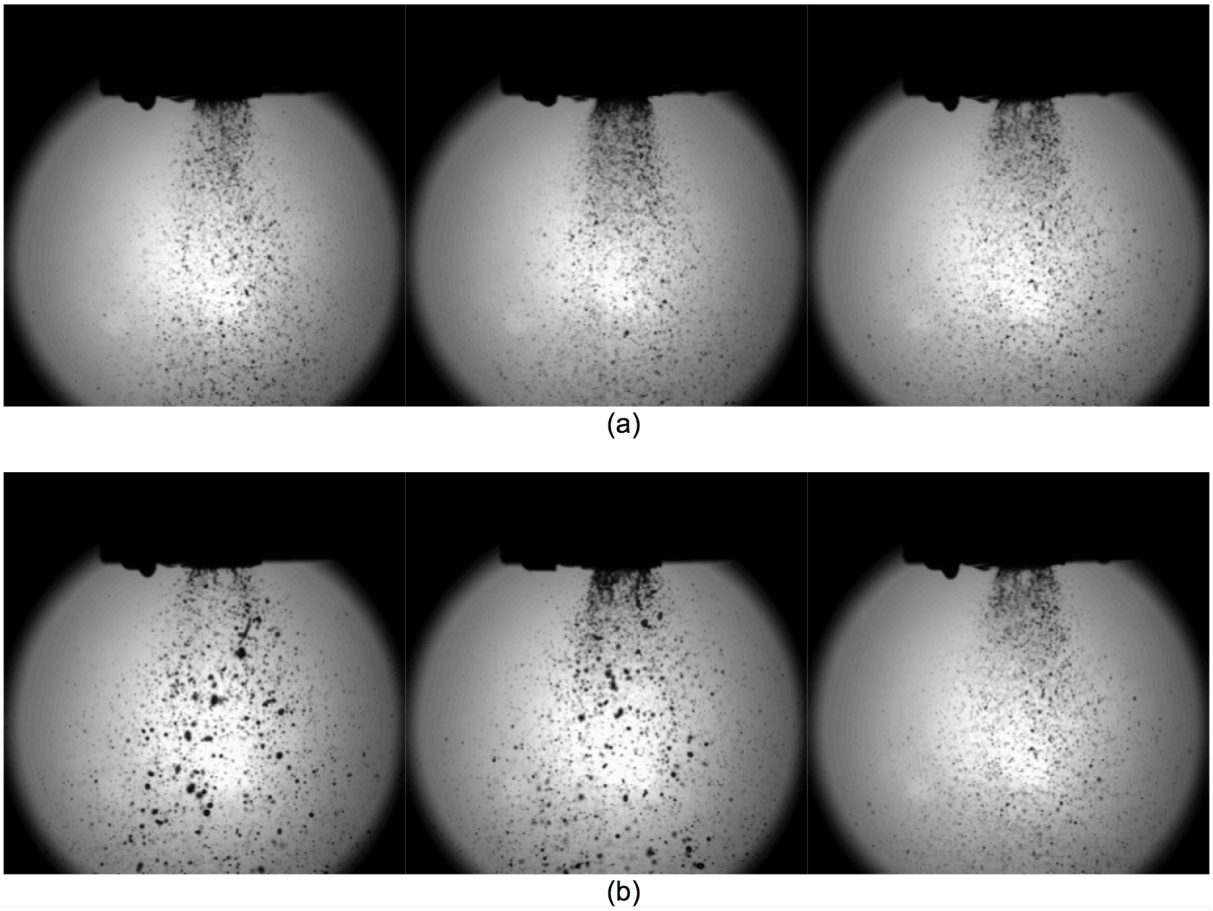

FIG. 4: Morphology of glycerol solution sprays (flow rate: 11 g/s). (a) Effect of rotation speed at fluid/N_2 ratio of 1.1; 1000 rpm (left), 1500 rpm (center), 2000 rpm (right). (b) Effect of N_2 flow rate at 2000 rpm; $G/N_2 = 2.15$ (left), $G/N_2 = 1.91$ (center), $G/N_2 = 1.1$ (right).

sprays; however, it failed to provide accurate results for Carbopol gel sprays, where larger drops may have significant radial velocity components due to centrifugal forces, which makes the definition of a cone angle very difficult.

3. RESULTS

3.1 Glycerol solution

The typical morphology of glycerol solution sprays is displayed in Figure 4, for different rotation speeds and different flow rates of the carrier gas. Unlike sprays generated by conventional nozzles, it is not possible to identify a primary atomization region surrounding a liquid core, because liquid breakup and mixing with the gas occurs inside the nozzle; this suggests the minimum standoff distance from the spray target can be very short. Increasing the rotation speed from 1000 rpm to 2000 rpm at constant nitrogen flow rate (Figure 4a) does not result into an appreciable change in the spray morphology, although one can observe

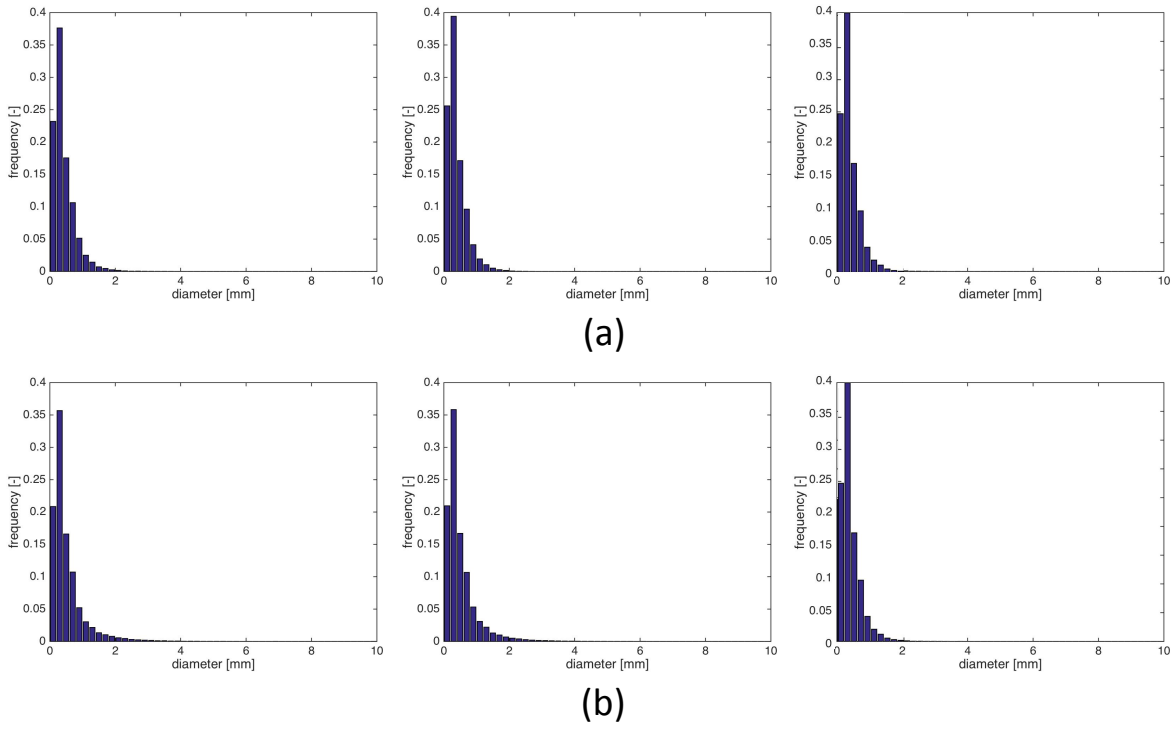

FIG. 5: Drop size distributions (discrete probability density of equivalent drop diameters) of glycerol solution sprays (flow rate: 11 g/s). (a) Effect of rotation speed at fluid/N_2 ratio of 1.1; 1000 rpm (left), 1500 rpm (center), 2000 rpm (right). (b) Effect of N_2 flow rate at 2000 rpm; $G/N_2 = 2.15$ (left), $G/N_2 = 1.91$ (center), $G/N_2 = 1.1$ (right).

a slightly more homogeneous granulometry, with a smaller number of larger drops. The effect of the nitrogen flow rate, shown in Figure 4b, is significantly more important, and one can clearly observe a reduction of the average drop size and a more homogeneous spray.

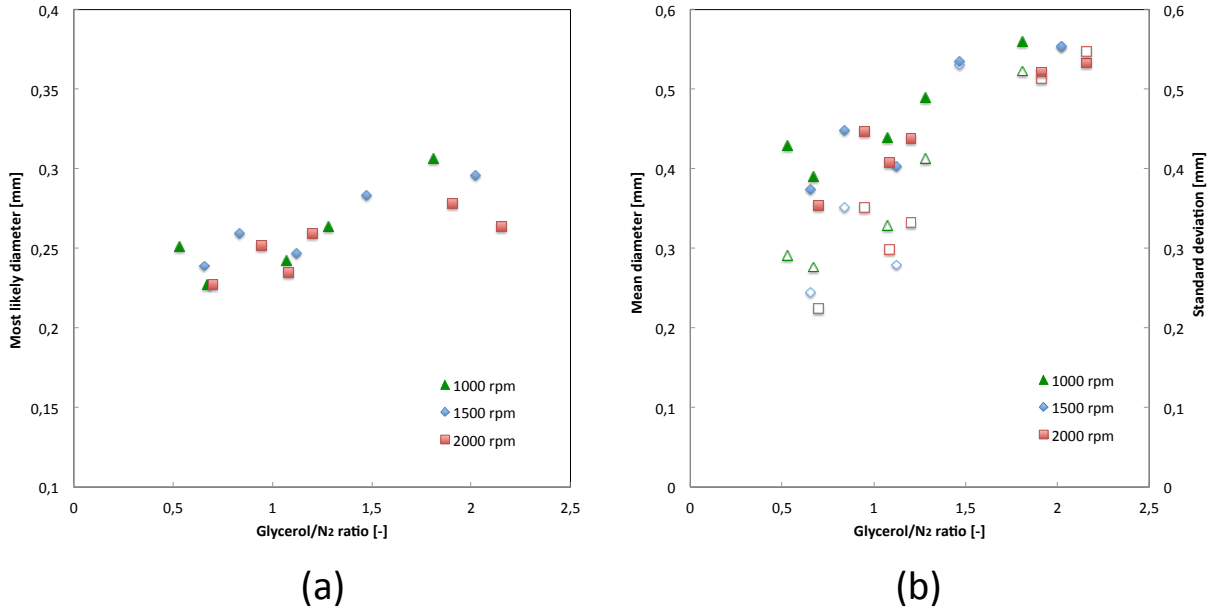

FIG. 6: Equivalent drop diameter for glycerol solution sprays as a function of the fluid/N_2 ratio: (a) most likely value; (b) average value (filled symbols) and standard deviation (open symbols).

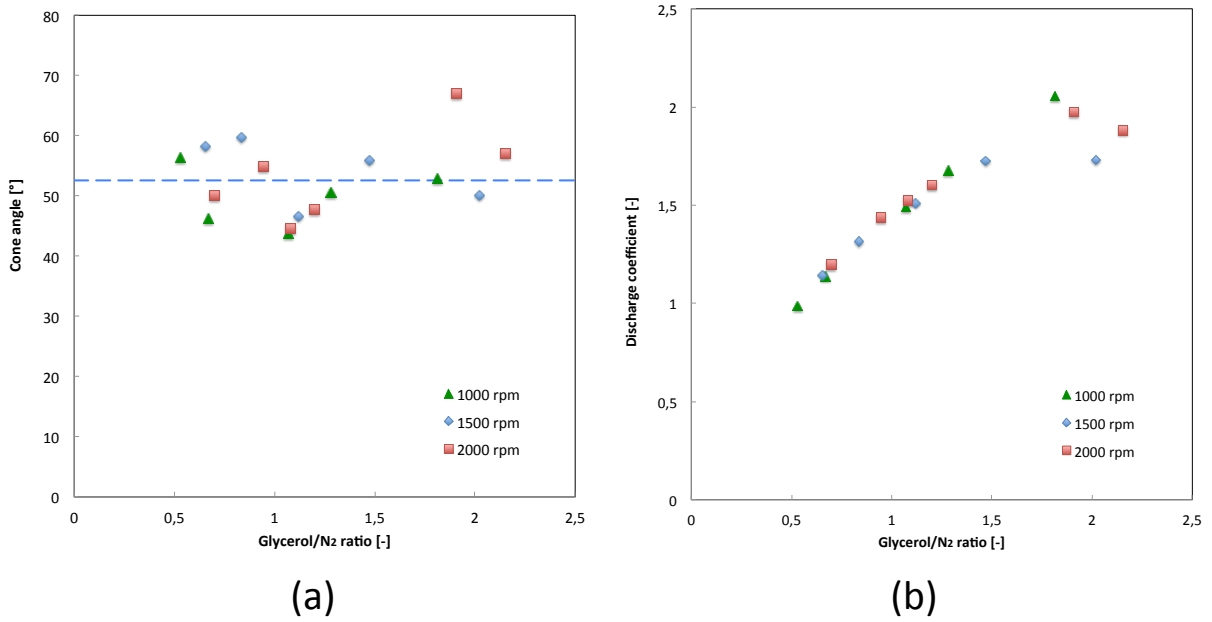

FIG. 7: Cone angle (a) and discharge coefficient (b) of the glycerol solution spray as a function of the fluid/N_2 ratio.

Figure 5 displays the drop size distribution histograms relative to the same experimental conditions of sprays in Figure 4. In all cases, distributions are unimodal, with the maximum frequency observed for equivalent diameters between 0.2 and 0.3 mm. Values of the most likely equivalent diameter and of the average diameter with its standard deviation are plotted in Figure 6 as a function of the glycerol/N_2 ratio; one can observe an increase of both the average and the most likely drop size with the glycerol/N_2 ratio, while the rotation speed does not seem to affect the drop size significantly within the range 1000–2000 rpm. For comparison, the diameter of a drop of the same fluid obtained from a monodisperse generator in the Rayleigh breakup regime would be:

$$d = 1.882(1 + \frac{3}{\sqrt{2}}Oh)^{\frac{1}{3}}D = 1.9mm \tag{2}$$

where $Oh = \eta/\sqrt{\rho\sigma D}$ is the Ohnesorge number and D is the nozzle diameter of the monodisperse generator.

The cone angle and the discharge coefficient, $C_D = \dot{m}_G/\rho_G A\sqrt{2\Delta P/\rho_G}$, where $\dot{m}_G$ and ρ_G are, respectively, the glycerol solution mass flow rate and density, A is the cross-sectional area of the nozzle outlet, and ΔP is the pressure drop across the nozzle, are displayed in Figure 7 as a function of the of the glycerol/N_2 ratio. The cone angle (Figure 7a) is approximately constant, with a mean value of $52°\pm6°$, and does not seem to be affected either by the fluid/gas ratio or by the rotation speed. The discharge coefficient exhibits a growing trend with respect to the fluid/gas ratio, which means sprays with finer atomisation (smaller drops) are also characterised by smaller discharge coefficients; the effect of the rotation speed is not significant in the range considered. The pressure drop is approximtely constant, with an average value of 250 ± 9 kPa.

Because of the peculiar atomization mechanism, and of the lack of experimental data in the same operating conditions, it is difficult to compare the proposed technology with other types of atomizers. A recent work reports measurements of glycerin atomization in a twin fluid nozzle with a much larger exit diameter (8 mm), for similar liquid and gas flow rates to those considered in the present work (García et al., 2017). In particular, droplet size distributions were measured with a Malvern Spraytec, equipped with a 450 mm lens adequate for diameters from 1 μm to 1 mm, as opposed to the present work where the digital image processing method used covered a range of equivalent drop diameters up to 10 mm, at the cost of a poorer resolution at smaller diameters (<500 μm). The reported values of the Sauter mean diameter in

the range between 15 μm and 1 mm, to be compared with mean diameters between 200 μm and 600 μm observed in the present work. However, a closer look at the droplet size distributions shows most of them are truncated in correspondence of the upper limit of the detector (1 mm), thus excluding all drops with a larger diameter.

3.2 Carbopol gel

The morphology of viscoplastic Carbopol gel sprays, shown in Figure 8, is significantly different from that of Newtonian glycerol solution sprays. These viscoplastic sprays are composed by a mixture of small spherical or ellipsoidal droplets and large chunks of fluid with irregular shapes (pseudo-drops), sometimes featuring elongated ligaments or dendrites. The presence of non-spherical, large drops is due to fluid yield

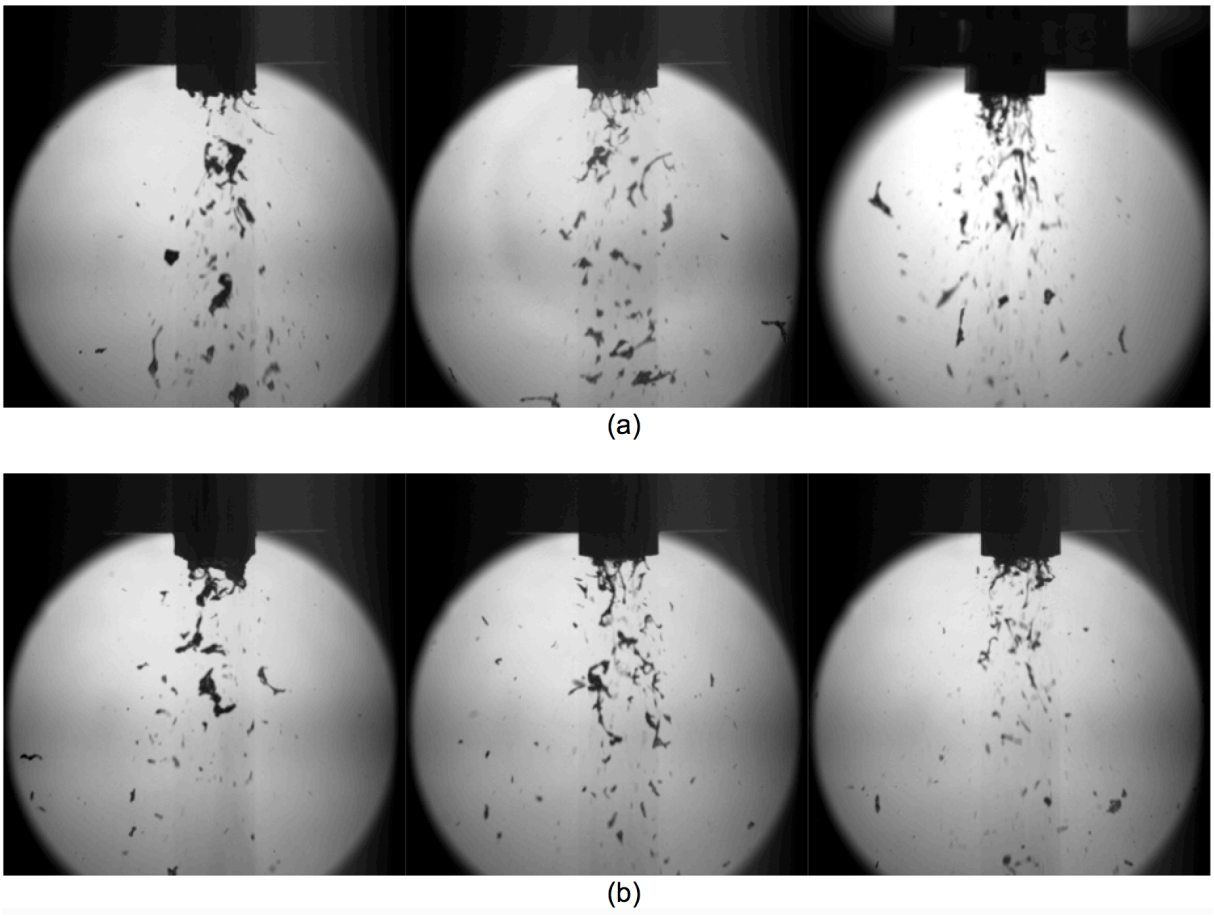

FIG. 8: Morphology of Carbopol gel sprays. (a) Effect of rotation speed at fluid/N_2 ratio of 2.4 and gel flow rate of 10 g/s; 1000 rpm (left), 1500 rpm (center), 2000 rpm (right). (b) Effect of N_2 flow rate at 2000 rpm and gel flow rate of 7 g/s; $G/N_2 = 2.09$ (left), $G/N_2 = 1.39$ (center), $G/N_2 = 1.28$ (right).

stress, which prevents the Laplace pressure from minimizing the surface energy of drops (proportional to the surface area) hence preventing the formation of spherical drops (German and Bertola, 2010a,b). The competition between the Laplace pressure and the yield stress is usually expressed by the Bingham-capillary number (Bertola, 2009):

$$\check{B} = \frac{\tau_0 d}{\sigma} \tag{3}$$

where τ_0 is the fluid yield stress, σ its surface tension, and d is a characteristic length. This number proved useful to characterise the flow of viscoplastic fluids in horizontal capillaries (Bertola, 2009), and the formation (German and Bertola, 2010a), free-fall (German and Bertola, 2010b), impact (Chen and Bertola, 2016) and spreading (German and Bertola, 2010c) of viscoplastic drops.

For values of $\check{B} < 1$, where the capillary pressure exceeds the yield stress of the fluid, the drop shapes are spherical, while for values of $\check{B} > 1$, where the yield stress is higher than the capillary pressure, the drop shape will be non-spherical, and is determined by the plastic deformation of the fluid due to the

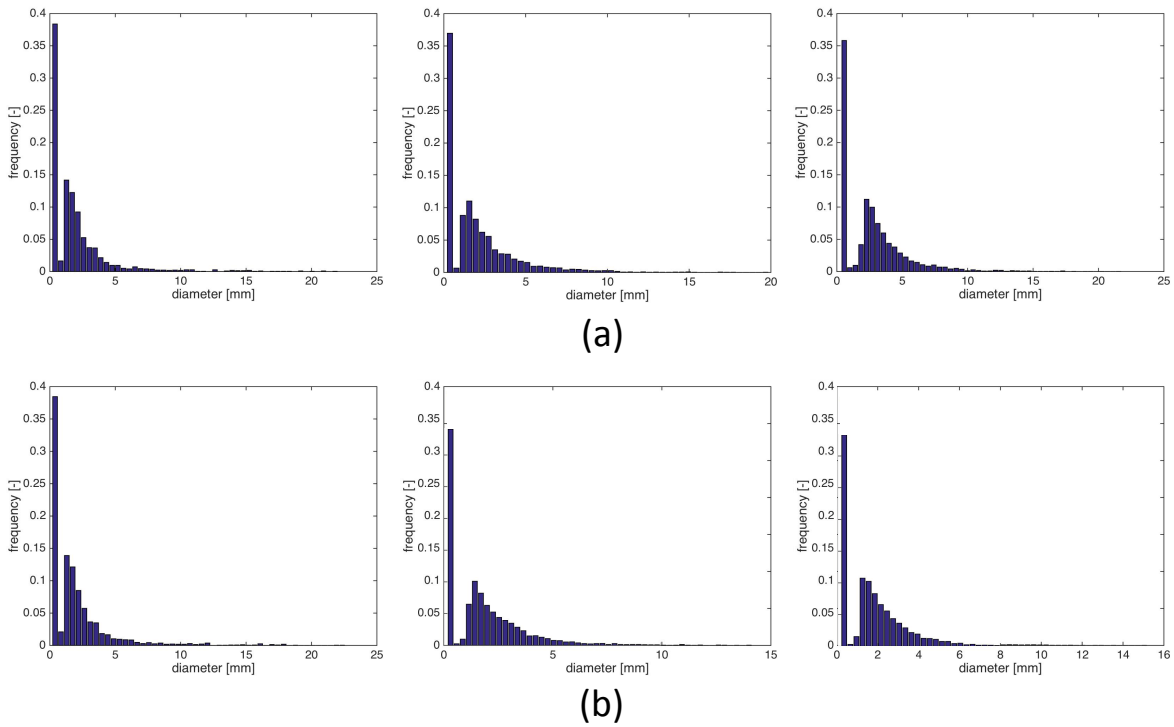

FIG. 9: Drop size distributions (discrete probability density of equivalent drop diameters) of Carbopol gel sprays. (a) Effect of rotation speed at fluid/N_2 ratio of 2.4 and gel flow rate of 10 g/s; 1000 rpm (left), 1500 rpm (center), 2000 rpm (right). (b) Effect of N_2 flow rate at 2000 rpm and gel flow rate of 7 g/s; $G/N_2 = 2.09$ (left), $G/N_2 = 1.39$ (center), $G/N_2 = 1.28$ (right).

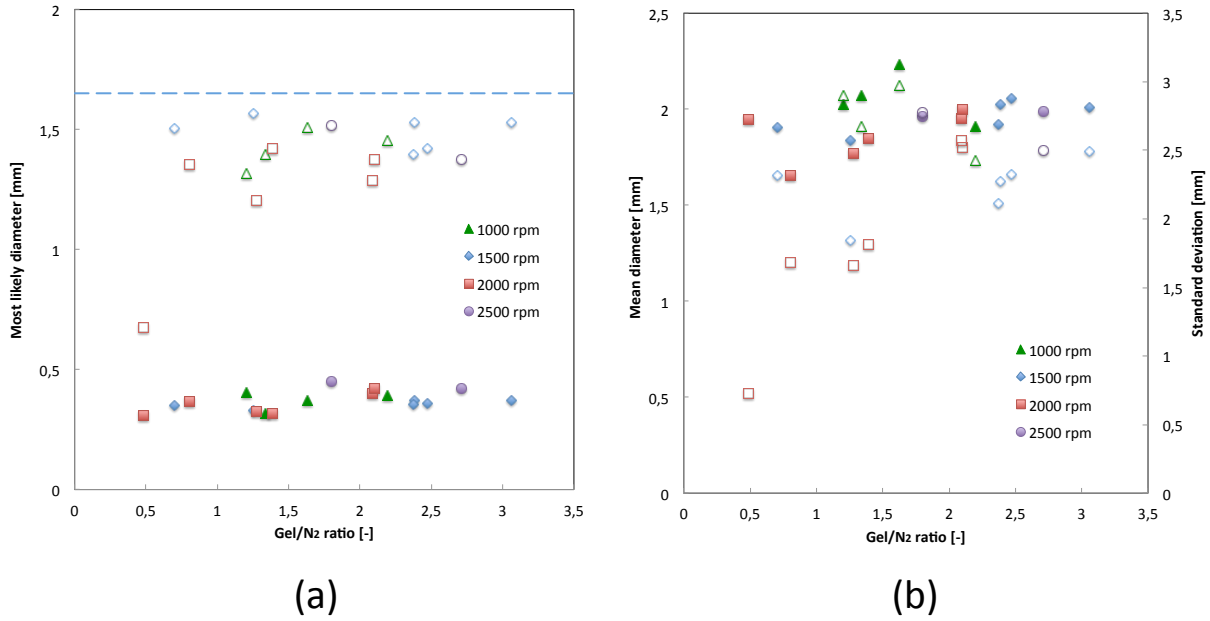

FIG. 10: Equivalent drop diameter for Carbopol gel sprays as a function of the fluid/N_2 ratio: (a) most likely value (filled symbols) and second most likely value (open symbols); (b) average value (filled symbols) and standard deviation (open symbols). The dashed line in (a) corresponds to the critical diameter ($\tilde{B} = 1$).

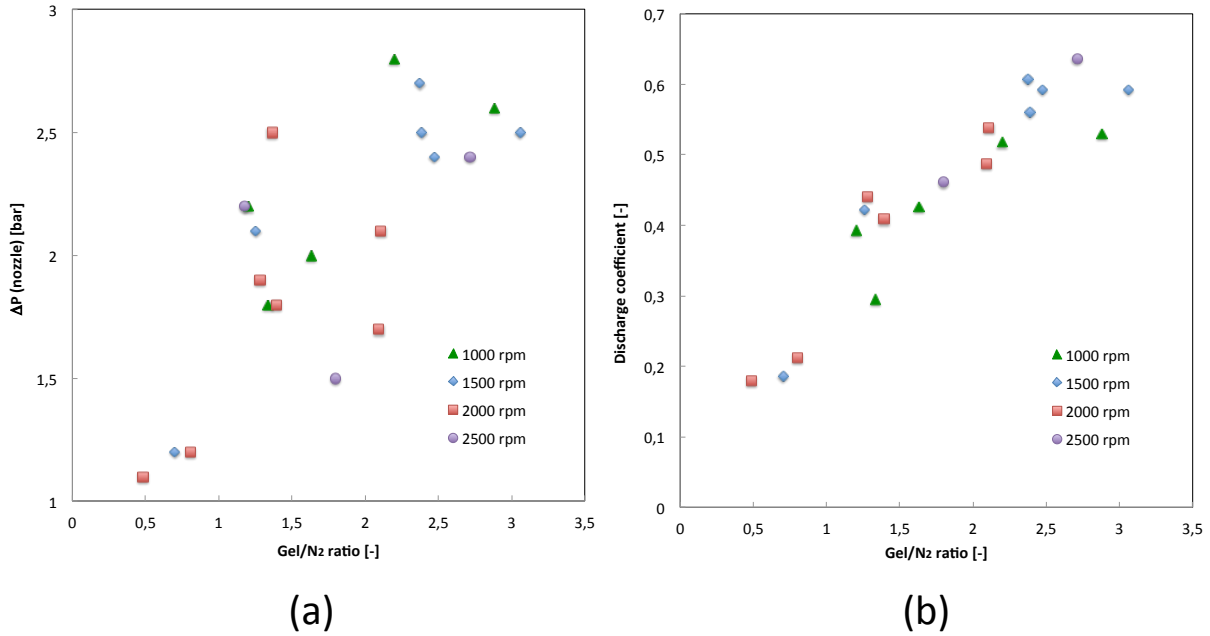

FIG. 11: Pressure drop across the nozzle (a) and discharge coefficient (b) of the Carbopol gel spray as a function of the fluid/N_2 ratio.

rotor and the aerodynamic force. With a yield stress of 60 Pa and a surface tension of 66 mN/m (Boujlel and Coussot, 2013), the minimum characteristic size of non-spherical pseudo-drops, calculated as $d = \sqrt[3]{6m/\pi\rho}$, is $d_{crit} = 1.1$ mm. Thus, for $d > d_{crit}$ the drop dynamics is dominated by the yield strss, and the only way to produce deformations eventually leading to breakup is to apply an external stress larger than the yield stress. In particular, surface instabilities cannot grow in amplitude, which inhibits the atomization process.

A qualitative analysis of Figure 8 suggests that both the rotor speed and the flow rate of the carrier gas affect the gel breakup, reducing the size of pseudo-drops; similar to the glycerol solution spray, the effect of the carrier gas flow rate is more significant. Another important feature one can observe in the images displayed in Figure 8 is that the spray is formed already at the nozzle exit, while in conventional atomization the primary breakup occurs at a certain distance from the nozzle even at high values of the Reynolds number. Figure 9 displays the drop size distribution histograms relative to the same experimental conditions of sprays in Figure 8. In contrast to the glycerol solution sprays, the drop size distributions of viscoplastic gel sprays are are bi-modal, with the maximum frequency observed for equivalent diameters between 0.2 and 0.3 mm, and a second relative maximum corresponding to larger bits of gel.

Figure 10 displays the most likely values (Figure 10a) and the average values (Figure 10b) of the equivalent drop diameter measured in Carbopol gel sprays as a function of the gel/N_2 ratio. The most likely value corresponding to the absolute maximum of the frequency distribution is approximately constant, while the values corresponding to the relative maximum are only weakly dependent on the gel/N_2. With one exception, observed at high N_2/gel ratio and high rotation speed, these values are just below the critical diameter calculated from Eq. (3) at the transition between the capillary regime and the viscoplastic regime ($\check{B} = 1$), which suggests the mixing process in the nozzle is effective in overcoming the yield stress and produces drops that are small enough to be in the capillary-driven regime. The pressure drop across the nozzle and the discharge coefficient, $C_D = \dot{m}_C/\rho_C A\sqrt{2\Delta P/\rho_C}$, where $\dot{m}_C$ and ρ_C are, respectively, the Carbopol gel mass flow rate and density, are displayed in Figure 11 as a function of the of the gel/N_2 ratio. Differently from the case of the glycerol solution, both the pressure drop and the discharge coefficient exhibit a growing trend with respect to the fluid/gas ratio, while the effect of the rotation speed is not significant. Sprays with finer atomisation (smaller drops) are characterised by discharge coefficients significantly smaller than those of the viscous Newtonian fluid.

4. CONCLUSIONS

A prototype air-blast rotary atomiser, based on the concept of a high-viscosity fluid emulsifier, was designed, built, and tested. Preliminary tests to provide a basic characterisation of the atomiser performance were conducted, using a viscous Newtonian fluid (glycerol-water), and a non-Newtonian viscoplastic fluid (Carbopol gel). It was demonstrated that the device is able to spray fluids with different physical properties, with relatively low pressure drops across the nozzle. This indicates the device has a good potential to find applications in the atomisation of high-viscosity and/or non-Newtonian fluids. Preliminary measurements of the spray cone angle and of the mean and modal drop diameters suggest that to achieve spray characteristics comparable to those of conventional nozzles, the device should be operated with high gas to liquid ratios and high rotation speeds.

ACKNOWLEDGMENTS

T.B. gratefully acknowledges financial support from DLR.

REFERENCES

Akay, G., Irving, G.N., Kowalski, A.J., and Machin, D., Dynamic mixing apparatus for the production of liquid compositions, February, 2002, uS6345907 B1.
URL www.google.com/patents/US6345907

Bertola, V., Wicking with a yield stress fluid, *Journal of Physics Condensed Matter*, vol. **21**, no. 3, 2009.

Bertola, V., Spraying device, July, 2016, registered Community Design 003307909-0001.
URL http://euipo.europa.eu/

Boujlel, J. and Coussot, P., Measuring the surface tension of yield stress fluids, *Soft Matter*, vol. **9**, pp. 5898–5908, 2013.

Brenn, G. and Plohl, G., The formation of drops from viscoelastic liquid jets and sheets - an overview, *Atomization and Sprays*, vol. **27**, no. 4, pp. 285–302, 2017.

Broniarz-Press, L., Ochowiak, M., and Woziwodzki, S., Atomization of {PEO} aqueous solutions in effervescent atomizers, *International Journal of Heat and Fluid Flow*, vol. **31**, no. 4, pp. 651 – 658, 2010.

Brown, C., Irving, G., and Kowalski, A., Mixing apparatus of the cddm- and/or ctm-type, and its use, May, 2012, uS20120113743 A1.
URL www.google.com/patents/US20120113743

Chen, S. and Bertola, V., The impact of viscoplastic drops on a heated surface in the leidenfrost regime, *Soft Matter*,

vol. **12**, no. 36, pp. 7624–7631, 2016, cited By 1.
URL

Clasen, C., Phillips, P.M., Palangetic, L., and Vermant, J., Dispensing of rheologically complex fluids: The map of misery, *AIChE Journal*, vol. **58**, no. 10, pp. 3242–3255, 2012.

Fuller, G.G. and Vermant, J., Complex fluid-fluid interfaces: Rheology and structure, *Annual Review of Chemical and Biomolecular Engineering*, vol. **3**, pp. 519–543, 2012.

García, J., Lozano, A., Alconchel, J., Calvo, E., Barreras, F., and Santolaya, J., Atomization of glycerin with a twin-fluid swirl nozzle, *International Journal of Multiphase Flow*, vol. **92**, pp. 150 – 160, 2017.
URL http://www.sciencedirect.com/science/article/pii/S0301932216307741

German, G. and Bertola, V., Formation of viscoplastic drops by capillary breakup, *Physics of Fluids*, vol. **22**, no. 3, p. 033101, 2010a.

German, G. and Bertola, V., The free-fall of viscoplastic drops, *Journal of Non-Newtonian Fluid Mechanics*, vol. **165**, no. 13-14, pp. 825–828, 2010b.

German, G. and Bertola, V., The spreading behaviour of capillary driven yield-stress drops, *Colloids and Surfaces A: Physicochemical and Engineering Aspects*, vol. **366**, no. 1-3, pp. 18–26, 2010c, cited By 8.
URL

Jorgensen, L., LeMerrer, M., Delanoë-Ayaria, H., and Barentin, C., Yield stress and elasticity influence on surface tension measurements, *Soft Matter*, vol. **11**, pp. 5111–5121, 2015.

Lin, S.P. and Reitz, R.D., Drop and spray formation from a liquid jet, *Annual Review of Fluid Mechanics*, vol. **30**, no. 1, pp. 85–105, 1998.

Mates, S. and Settles, G., A study of liquid metal atomization using close-coupled nozzles, part 1: Gas dynamic behavior, *Atomization and Sprays*, vol. **15**, no. 1, pp. 19–40, 2005.

Negri, M. and Ciezki, H.K., Atomization of viscoelastic fluids with an impinging jet injector: Morphology and physical mechanism of thread formation, *Atomization and Sprays*, vol. **27**, no. 4, pp. 319–336, 2017.

Negri, M., Ciezki, H.K., and Schlechtriem, S., Spray behavior of non-newtonian fluids: correlation between rheological measurements and droplets/threads formation, , 2013.
URL https://doi.org/10.1051/eucass/201304271

Otsu, N., A threshold selection method from gray-level histograms, *IEEE Transactions on Systems, Man, and Cybernetics*, vol. **9**, pp. 66–66, 1979.

Plog, J., Kulicke, W.M., and Clasen, C., Influence of the molar mass distribution on the elongational behaviour of polymer solutions in capillary breakup, *Applied Rheology*, vol. **15**, pp. 28–37, 2005.

Rahimi, S. and Natan, B., Atomization of gel propellants through an air-blast triplet atomizer, *Atomization and Sprays*, vol. **16**, no. 4, pp. 379–400, 2006.

Rogers, G. and Barnes, H., New measurements of the flow–curves for carbopol dispersions without slip artefacts, *Rheologica Acta*, vol. **40**, pp. 499–503, 2001.

Schütz, S., Breitling, M., and Piesche, M., Atomization of suspensions with shear-thinning behavior by aerodynamic wave breakup, *Chemical Engineering Technology*, vol. **27**, no. 6, pp. 619–624, 2004.

Smith, M., Besseling, R., Cates, M., and Bertola, V., Dilatancy in the flow and fracture of stretched colloidal suspensions, *Nature Communications*, vol. **1**, pp. 114–118, 2010.

Thompson, J.C. and Rothstein, J.P., The atomization of viscoelastic fluids in flat-fan and hollow-cone spray nozzles, *Journal of Non-Newtonian Fluid Mechanics*, vol. **147**, pp. 11–22, 2007.

Yang, L., Fu, Q., Qu, Y., Zhang, W., Du, M., and Xu, B., Spray characteristics of gelled propellants in swirl injectors, *Fuel*, vol. **97**, pp. 253–261, 2012.